



Negative magnetostrictive magnetoelectric coupling of BiFeO₃

Sanghyun Lee,^{1,2,3} M. T. Fernandez-Diaz,⁴ H. Kimura,⁵ Y. Noda,⁵ D. T. Adroja,⁶ Seongsu Lee,⁷ Junghwan Park,^{2,3} V. Kiryukhin,⁸ S.-W. Cheong,⁸ M. Mostovoy,⁹ and Je-Geun Park^{1,2,10,*}

¹Center for Functional Interfaces of Correlated Electron Systems, Institute for Basic Science, Seoul National University, Seoul 151-747, Korea

²Center for Strongly Correlated Materials Research, Seoul National University, Seoul 151-742, Korea

³Department of Physics, SungKyunKwan University, Suwon 440-746, Korea

⁴Institut Laue-Langevin, Boîte Postale 156, 38042 Grenoble Cedex, France

⁵Institute of Multidisciplinary Research for Advanced Materials, Tohoku University, Sendai 980-8577, Japan

⁶ISIS Facility, Rutherford Appleton Laboratory, Chilton, Didcot, Oxon OX11 0QX, United Kingdom

⁷Neutron Science Division, Korea Atomic Energy Research Institute, Daejeon 305-353, Korea

⁸Rutgers Center for Emergent Materials and Department of Physics and Astronomy, Rutgers University, Piscataway, New Jersey 08854, USA

⁹Zernike Institute for Advanced Materials, University of Groningen, Nijenborgh 4, 9747 AG, Groningen, The Netherlands

¹⁰FPRD, Department of Physics & Astronomy, Seoul National University, Seoul 151-747, Korea

(Received 1 June 2013; published 21 August 2013)

How magnetoelectric coupling actually occurs on a microscopic level in multiferroic BiFeO₃ is not well known. By using high-resolution single crystal neutron diffraction techniques, we have determined the electric polarization of each individual element of BiFeO₃, and concluded that magnetostrictive coupling suppresses the electric polarization at the Fe site below T_N . This negative magnetoelectric coupling appears to outweigh the spin current contributions arising from the cycloid spin structure, which should produce positive magnetoelectric coupling.

DOI: 10.1103/PhysRevB.88.060103

PACS number(s): 75.85.+t, 61.05.F–, 75.50.Ee

Multiferroic materials with a coexistence of both ferroelectricity and magnetism offer a huge potential and, at the same time, pose new challenges for our understanding of how magnetism and ferroelectricity can be coupled to one another in real materials.^{1,2} Once fully achieved, this understanding of their coupling, the so-called magnetoelectric effects, can lead to better manipulation of unusual multiferroic behavior. However, one needs to carry out precise measurements of both the structure and dynamics in order to gain a fundamental understanding of the underlying physics. Despite the academic and technological importance, however, the origin of magnetoelectric coupling has proven to be often challenging to address experimentally for a given material.

BiFeO₃ is arguably one of the most extensively studied multiferroic materials with several distinctive properties.^{3–5} For example, it has both magnetic and ferroelectric phase transitions above room temperature, $T_N = 650$ K and $T_C = 1100$ K. Moreover, it has one of the largest reported values ever of polarization, ~ 86 $\mu\text{C}/\text{cm}^2$, with the noncentrosymmetric space group of $R3c$ in the ferroelectric phase, as shown in Fig. 1(a). However, how magnetoelectric coupling actually occurs and moreover how to understand it remains to be resolved. Another interesting point to be noted is that when it undergoes basically a G -type magnetic ordering at 650 K, an incommensurate structure is formed with an extremely long period of 620 Å due to the Dzyaloshinski-Moriya (DM) interaction without breaking the crystal symmetry [see Figs. 1(b) and 1(c)].⁶ In hexagonal notation, the propagation vector of the incommensurate structure is $\mathbf{Q} = [0.0045, 0.0045, 0]$ at room temperature with a chiral vector of $\mathbf{e}_3 = [-1 \ 1 \ 0]$. The spin waves of BiFeO₃ measured by inelastic neutron scattering techniques^{7,8} are consistent with a Heisenberg Hamiltonian with a DM interaction, which was derived from bulk measurements.⁹

As regards magnetoelectric coupling, multiferroic materials with chiral magnetic structures offer an interesting, as yet unexplored, possibility for inverse DM effects. This inverse DM effect induces an electric polarization when a particular chiral structure sets in.¹⁰ The underlying mechanism of such additional polarization has been theoretically investigated by several groups.^{11,12} Another equally viable scenario is the more classical mechanism of lattice-mediated spin-lattice coupling. Few systematic studies have so far been made in which one of the two mechanisms works for BiFeO₃.

Here, we present detailed experimental measurements of magnetoelectric coupling in BiFeO₃ by using high-resolution single crystal neutron diffraction techniques. Through close examination of the temperature-dependent electric polarizations by Bi and Fe atoms, we demonstrate that magnetostrictive magnetoelectric coupling suppresses the polarization of Fe in the magnetically ordered phase, outweighing that due to the inverse DM effect.

High-resolution single crystal neutron diffraction experiments were carried out using a neutron wavelength of 0.835 Å from 300 to 850 K at the D9 diffractometer of the ILL, France. We used single crystals grown by a flux method with a typical size of $1.6 \times 2.6 \times 2.4$ mm³. We have carried out all our analysis using the FULLPROF program.¹³

BiFeO₃ of the $R3c$ space group undergoes an incommensurate antiferromagnetic transition at $T_N = 650$ K with a cycloid magnetic structure as shown in Fig. 1(a). Because of the threefold rotational symmetry along the c axis, there are three equivalent propagation vectors for the cycloid magnetic structure with $\mathbf{Q}_1 = [1 \ 1 \ 0]$, $\mathbf{Q}_2 = [-2 \ 1 \ 0]$, and $\mathbf{Q}_3 = [1 \ -2 \ 0]$, and they are thermally populated as separate magnetic domains, as seen by polarized neutron diffraction experiments.¹⁴ There are two possible directions of spin rotation for each of the three \mathbf{Q} vectors, which are related

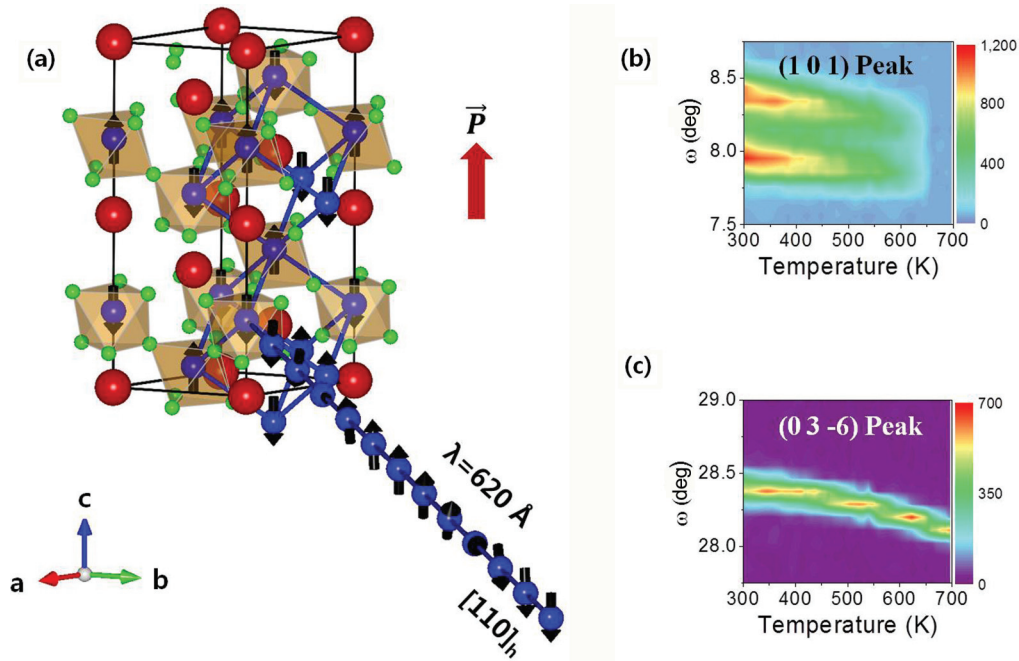


FIG. 1. (Color online) (a) Cycloid magnetic structure of BiFeO_3 with the propagation vector Q along the $[1\ 1\ 0]$ direction. In this hexagonal setting, the total ferroelectric polarization (P) is pointing along the c axis. (b) and (c) show the temperature dependence of magnetic $(1\ 0\ 1)$ and nuclear $(0\ 3\ -6)$ Bragg peaks.

to the aforementioned DM interaction. For example, the spin chiral vector e_1 parallel to the $[-1\ 1\ 0]$ axis produces a clockwise rotation of the cycloid structure while e_2 parallel to the $[1\ -1\ 0]$ axis does an anticlockwise rotation, when the cycloid structure is viewed on the (hhl) plane. A recent x-ray scattering experiment with polarization analysis shows that the sense of the spin rotation is clockwise.¹⁵

This clockwise spin rotation can then give rise to an induced electric polarization ΔP via the inverse DM effect. This additional electric polarization can be written in the following form, $\Delta P = Ae \times Q$, where A is a material specific coefficient, e is the spin-rotation chiral vector, and Q is the propagation vector of the chiral magnetic structure.¹² Furthermore, it is important to note that a Ginzburg-Landau analysis based on the symmetry of BiFeO_3 predicts that ΔP should be parallel to the total polarization direction in the paramagnetic phase, i.e., positive ΔP . In our calculation, the total electric polarization (P) always points along the c axis above T_N . Notice that this dependence of ΔP due to the inverse DM effect is equally valid for the other two Q vectors. On the other hand, magnetoelectric coupling of a magnetostrictive nature can produce negative ΔP . Therefore, one can precisely determine which one of the two mechanisms is at work for BiFeO_3 simply by measuring ΔP below T_N .

This realization opens up a simple yet elegant way of addressing the issue of magnetoelectric coupling in BiFeO_3 . In fact, we have tried to answer this question by carrying out high-resolution structure studies before, where we noted a quite significant change in the lattice constants below T_N .¹⁶ However, because of technical limitations in our previous diffraction experiments, we had to make most of our analysis then using synchrotron data. More specifically, we could not examine the temperature-dependent contributions to the

electric polarization by individual elements because of the lack of accurate information about the O positions over the entire temperature range: X-ray data are typically less sensitive to lighter elements such as O as compared to neutrons.

In order to overcome these previous technical difficulties, we have now carried out higher-resolution single crystal neutron diffraction experiments using the D9 beamline. We have taken special efforts to increase the number of nuclear peaks by a factor of 2 as compared with the previous experiment as well as to measure the data over a very wide temperature range, in particular, extending the temperature range above T_N .

Let us first explain the aim of the experiment from a crystallographic viewpoint. To estimate the individual electric polarization by Bi and Fe atoms, we have assumed the high temperature paraelectric phase of the $Pm\text{-}3m$ space group. Although the ferroelectric transition and the space group of the paraelectric phase are still under debate,^{17,18} one of the proposed candidates is the $Pbnm$ orthorhombic structure (see Fig. 2), and our analysis and conclusion below are valid regardless of the nature of the ferroelectric transition since we are only concerned here with temperature-induced electric polarization. With the paraelectric phase of $Pm\text{-}3m$, the electric polarization by individual atoms can be calculated by simply measuring the relative shifts of Fe and Bi atoms with respect to the center of the oxygen octahedron. For more simplicity, we can take the relative shift of Fe and Bi atoms from their original positions in the paraelectric phase. Since the space group $R3c$ has an uncertain origin from a crystallographic viewpoint, usually $\text{Bi}(z)$ is fixed as an origin. However, in this Rapid Communication we consider the shift of Bi and Fe atoms relative from the oxygen atom, thus we fixed the z position of the oxygen as an origin (see Fig. 2).

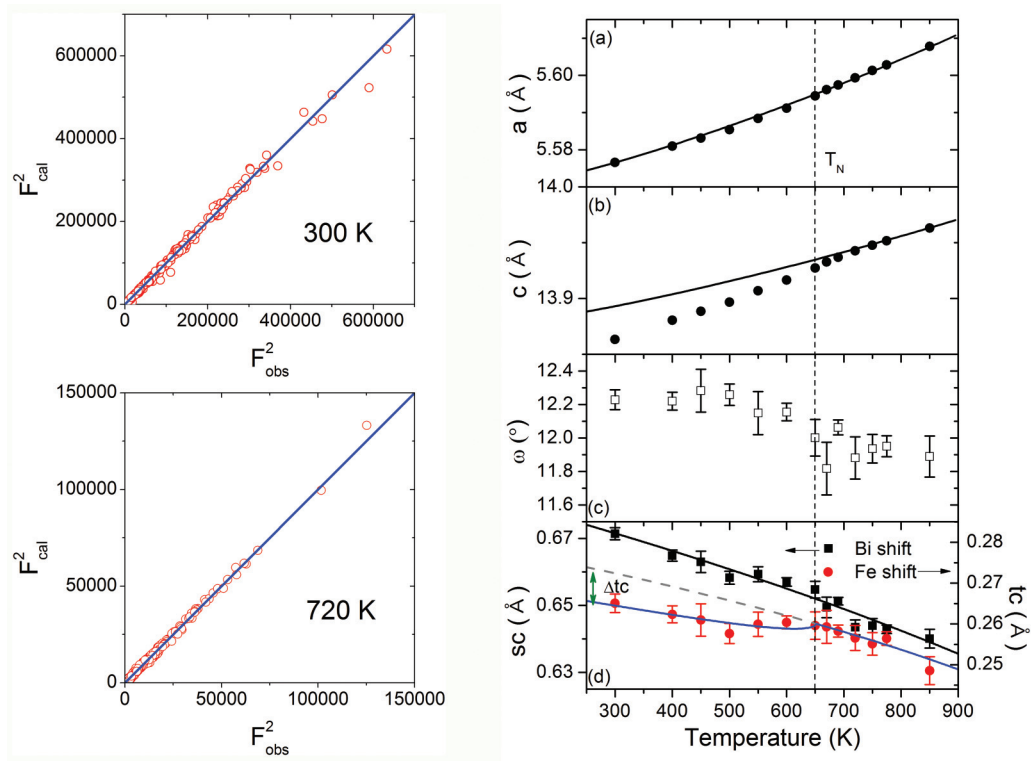


FIG. 3. (Color online) Left: Calculated and observed squared structure factor at two representative temperatures of 300 and 720 K with 222 and 218 nuclear Bragg peaks, respectively. Right: The temperature dependence is shown of the lattice constants [(a) and (c)] together with the antiphase rotation angle ω of the oxygen octahedron in addition to the Bi (sc) and Fe (tc) shifts along the c axis. The solid lines in (a) and (b) represent our theoretical calculations using a Debye-Grüneisen formula as in the text, while the solid lines in (d) represent the theoretical temperature dependence of the first-order ferroelectric order parameter based on the Ginzburg-Landau free energy analysis with the magnetoelectric coupling term, as discussed in the text. The dashed line plots the theoretical calculation results of the Fe shift (tc) without the magnetoelectric term.

measured intensity of the $(0\ 0\ 3) \pm Q$ magnetic superlattice peak in Fig. 4. With this information, we also reanalyzed our previous data taken from another single crystal diffractometer (FONDER), and present them in Fig. 4 together with the theoretical line as discussed above. As can be seen, both sets of our

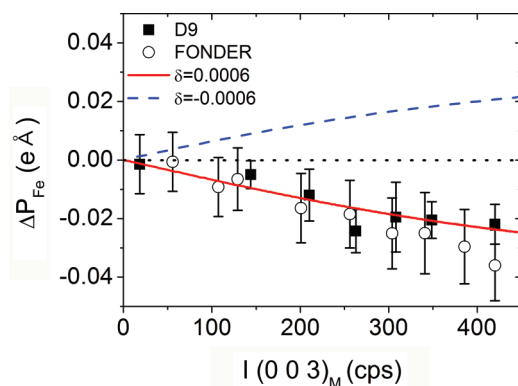


FIG. 4. (Color online) Plot of the induced electric polarization of Fe (ΔP_{Fe}) against the measured intensity of the $(0\ 0\ 3) \pm Q$ magnetic superlattice peaks. The solid line represents the theoretical calculation results based on the Ginzburg-Landau free energy analysis with a negative magnetoelectric coupling as discussed in the text, while the dashed line shows the theoretical results expected for the case with the opposite sign for the magnetoelectric coupling.

data from the two different instruments display ΔP_{Fe} , which is in good agreement with one another. It is also consistent with the theoretical calculations of the GL free energy with negative magnetostrictive magnetoelectric coupling, i.e., a positive sign of δ in our Ginzburg-Landau functional. We should note that our results cannot be reconciled by theoretical calculations with an opposite sign of magnetoelectric coupling, as shown by the dashed line in Fig. 4.

We note that our observation of the overall negative magnetoelectric coupling is qualitatively consistent with the field-induced electric polarization observed experimentally.^{16,21,22} Notice that all previous pyroelectric current measurements only measured the absolute value of ΔP , not its sign for the intrinsic technical problems. However, we acknowledge there is a discrepancy at a quantitative level. For example, our estimated value of ΔP is ~ 400 nC/cm² while the bulk value was reported to be ~ 40 nC/cm².^{16,21} It may well be plausible that our experimental values of the electric polarization might overestimate the magnetoelectric effect. We make one passing comment which has much wider implications: Our works and the conclusion made here suggest that it should be a very useful exercise for one to examine the origin of magnetoelectric coupling by using high-resolution diffraction studies as we have done for BiFeO₃ here.

In summary, we have experimentally determined the origin of magnetoelectric coupling in BiFeO₃ by high-resolution

single crystal neutron diffraction studies. Our calculation of the induced electric polarization of each Fe and Bi in the magnetic phase demonstrates that magnetoelectric coupling of the magnetostrictive origin suppresses the electric polarization at the Fe site below T_N , outweighing that of the inverse Dzyaloshinskii-Moriya effects, and becomes the dominant magnetoelectric coupling mechanism for BiFeO₃.

We thank N. Nagaosa, P. Radaelli, and R. Johnson for helpful discussions. This work was supported by the Research Center Program of IBS (Institute for Basic Science/Grant No. EM1203) in Korea and by the National Research Foundation of Korea (Grant No. R17-2008-033-01000-0). The work at Rutgers is supported by the U.S. Department of Energy under Contract No. DE-FG02-07ER46382.

*jgpark10@snu.ac.kr

¹M. Fiebig, *J. Phys. D* **38**, R123 (2005).

²W. Eerenstein, N. D. Mathur, and J. F. Scott, *Nature (London)* **442**, 759 (2006).

³J. Wang, J. B. Neaton, H. Zheng, V. Nagarajan, S. B. Ogale, B. Liu, D. Viehland, V. Vaithyanathan, D. G. Schlom, U. V. Waghmare, N. A. Spaldin, K. M. Rabe, M. Wuttig, and R. Ramesh, *Science* **299**, 1719 (2003).

⁴T. Choi, S. Lee, Y. J. Choi, V. Kiryukhin, and S.-W. Cheong, *Science* **324**, 63 (2009).

⁵J. B. Neaton, C. Ederer, U. V. Waghmare, N. A. Spaldin, and K. M. Rabe, *Phys. Rev. B* **71**, 014113 (2005).

⁶I. Sosnowska, T. Peterlin-Neumaier, and E. Steichele, *J. Phys. C* **15**, 4835 (1982).

⁷J. Jeong, E. A. Goremychkin, T. Guidi, K. Nakajima, G. S. Jeon, S. A. Kim, S. Furukawa, Y. B. Kim, S. Lee, V. Kiryukhin, S.-W. Cheong, and J. G. Park, *Phys. Rev. Lett.* **108**, 077202 (2012).

⁸M. Matsuda, R. S. Fishman, T. Hong, C. H. Lee, T. Ushiyama, Y. Yanagisawa, Y. Tomioka, and T. Ito, *Phys. Rev. Lett.* **109**, 067205 (2012).

⁹K. Ohoyama, S. Lee, S. Yoshii, Y. Narumi, T. Morioka, H. Nojiri, G. S. Jeon, S.-W. Jeon, and J.-G. Park, *J. Phys. Soc. Jpn.* **80**, 125001 (2011).

¹⁰S.-W. Cheong and M. Mostovoy, *Nat. Mater.* **6**, 13 (2007).

¹¹H. Katsura, N. Nagaosa, and A. V. Balatsky, *Phys. Rev. Lett.* **95**, 057205 (2005).

¹²I. A. Sergienko and E. Dagotto, *Phys. Rev. B* **73**, 094434 (2006).

¹³J. Rodriguez-Carvajal, *Physica B* **192**, 55 (1993).

¹⁴S. Lee, T. Choi, W. Ratcliff II, R. Erwin, S.-W. Cheong, and V. Kiryukhin, *Phys. Rev. B* **78**, 100101(R) (2008).

¹⁵R. D. Johnson, P. Barone, A. Bombardi, R. J. Bean, S. Picozzi, P. G. Radaelli, Y. S. Oh, S.-W. Cheong, and L. C. Chapon, *Phys. Rev. Lett.* **110**, 217206 (2013).

¹⁶J. Park, S.-H. Lee, S. Lee, F. Gozzo, H. Kimura, Y. Noda, Y. J. Choi, V. Kiryukhin, S.-W. Cheong, Y. Jo, E. S. Choi, L. Balicas, G. S. Jeon, and J.-G. Park, *J. Phys. Soc. Jpn.* **80**, 114714 (2011).

¹⁷S. M. Selbach, T. Tybell, M.-A. Einarsrud, and T. Grande, *Adv. Mater.* **20**, 3692 (2008).

¹⁸D. C. Arnold, K. S. Knight, F. D. Morrison, and P. Lightfoot, *Phys. Rev. Lett.* **102**, 027602 (2009).

¹⁹See Supplemental Material at <http://link.aps.org/supplemental/10.1103/PhysRevB.88.060103> for a summary of the crystal structure.

²⁰S. Lee, A. Pirogov, M. Kang, K.-H. Jang, M. Yonemura, T. Kamiyama, S.-W. Cheong, F. Gozzo, N. Shin, H. Kimura, Y. Noda, and J.-G. Park, *Nature (London)* **451**, 805 (2008).

²¹M. Tokunaga, M. Azuma, and Y. Shimakawa, *J. Phys. Soc. Jpn.* **79**, 064713 (2010).

²²A. M. Kadomtseva, A. K. Zvezdin, Yu. F. Popov, A. P. Pyatakov, and G. P. Vorob'ev, *JETP Lett.* **79**, 571 (2004).